



NRC Publications Archive Archives des publications du CNRC

Evaluation of corrosion of reinforcement in repaired concrete

Qian, S. Y.; Chagnon, N.

This publication could be one of several versions: author's original, accepted manuscript or the publisher's version. /
La version de cette publication peut être l'une des suivantes : la version prépublication de l'auteur, la version acceptée du manuscrit ou la version de l'éditeur.

NRC Publications Record / Notice d'Archives des publications de CNRC:

<https://nrc-publications.canada.ca/eng/view/object/?id=64db226b-39e1-4489-ac54-15dd8f7c2dd0>

<https://publications-cnrc.canada.ca/fra/voir/objet/?id=64db226b-39e1-4489-ac54-15dd8f7c2dd0>

Access and use of this website and the material on it are subject to the Terms and Conditions set forth at

<https://nrc-publications.canada.ca/eng/copyright>

READ THESE TERMS AND CONDITIONS CAREFULLY BEFORE USING THIS WEBSITE.

L'accès à ce site Web et l'utilisation de son contenu sont assujettis aux conditions présentées dans le site

<https://publications-cnrc.canada.ca/fra/droits>

LISEZ CES CONDITIONS ATTENTIVEMENT AVANT D'UTILISER CE SITE WEB.

Questions? Contact the NRC Publications Archive team at

PublicationsArchive-ArchivesPublications@nrc-cnrc.gc.ca. If you wish to email the authors directly, please see the first page of the publication for their contact information.

Vous avez des questions? Nous pouvons vous aider. Pour communiquer directement avec un auteur, consultez la première page de la revue dans laquelle son article a été publié afin de trouver ses coordonnées. Si vous n'arrivez pas à les repérer, communiquez avec nous à PublicationsArchive-ArchivesPublications@nrc-cnrc.gc.ca.





NRC - CNRC

Evaluation of corrosion of reinforcement in repaired concrete

Qian, S.Y.; Chagnon, N.

NRCC-39305

A version of this paper is published in / Une version de ce document se trouve dans :
9th International Conference and Exhibition, Structural Faults and Repair, London, UK.,
4-6 July 2001, pp. 1-12

www.nrc.ca/irc/ircpubs



EVALUATION OF CORROSION OF REINFORCEMENT IN REPAIRED CONCRETE

Shiyuan Qian and N. Chagnon
Urban Infrastructure Rehabilitation
Institute for Research in Construction
National Research Council Canada
M-20, Montreal Road, Ottawa, Ontario, Canada K1A 0R6

KEYWORDS: Concrete, Bridges, Corrosion, Reinforcing steel, half-cell potential.

ABSTRACT

Corrosion of steel in concrete is a complex phenomenon affected by many environmental factors. A reliable and effective non-destructive approach for assessing and predicting the state of reinforcement corrosion in concrete has not yet been developed. Current methods do not account for the effects of prevailing environmental conditions. Half-cell potential, linear polarization and concrete resistivity measurements are sensitive to the ambient environment, especially oxygen and water in concrete. Completely water-saturated concrete, for instance, can lead to oxygen starvation, resulting in corrosion potential and current values that are lower than normally expected and provide, therefore, a poor prediction of the corrosion state.

This paper presents the results of a study of the reinforcement corrosion in repaired concrete slabs taken from an old bridge in Hawkesbury, Ontario and additional results measured on electrochemical cells. Each corrosion measurement technique has its specific characteristics and limitations. The investigation showed that a better and more reliable prediction could be obtained by analyzing the data from above measurements jointly by considering the effects of environmental conditions.

INTRODUCTION

A large number of highway bridges are made of reinforced concrete and have shown serious deterioration due to corrosion of reinforcement, particularly those over 20 years of age. Extensive bridge deterioration can affect their safety and serviceability and result in loss of life or injury, traffic disruption and high user costs.

The deterioration of concrete bridge structures caused by corrosion of the reinforcement is due to the breakdown of the passive film (a thin but dense protective oxide film on the steel surface). This breakdown is caused either by carbonation or by chloride attack. Carbonation of concrete is the result of the reaction between atmospheric carbon dioxide and both calcium hydroxide and calcium silicate hydrates. CO_2 dissolves in the pore water and forms carbonic acid, which reduces the pH to a level at which the passive layer on the steel reinforcement is no longer sustained. Sulfur dioxide and nitrogen dioxide in the air also significantly reduce the pH of the pore water and cause structures to deteriorate. Chloride attack is a direct attack upon the passive layer of the reinforcement. When the chloride to hydroxyl ion ratio exceeds a certain level, chloride ions will break down the passive layer and cause localized corrosion. Chloride attack is the main cause of bridge corrosion in North America because this situation is severe when deicing salts are applied intensively. When embedded steel corrodes, the production of voluminous corrosion products induces internal stresses in the concrete surrounding the reinforcement. The internal tensile stresses eventually exceed the concrete tensile strength leading to cracking and spalling of the concrete cover.

The use of half-cell potential measurements for the detection of corrosion in reinforcing steel bars in concrete has been frequently employed since the early 1980's. This method provides an indication of the relative probability of corrosion activity through measurement of the potential difference between a

standard portable reference and the reinforcing steel, but it is unable to determine corrosion rates or the degree of corrosion that has occurred. The data analysis guidelines described in ASTM C876 (ASTM C876-99) provide general principles for the evaluation of corrosion probability of reinforcing steel in concrete. In many cases, the predicted corrosion state based on the guidelines are quite different from the actual corrosion conditions. A large discrepancy between the condition assessment and the actual deterioration has been observed in many bridges when they are about to undergo repair (Elsener & Bohni, 1990). The ASTM guidelines don't account for the many factors, such as oxygen and chloride concentrations, temperature and moisture content, etc. that can affect half-cell potentials over a certain range. Studies on European bridge decks (Raherinaivo, 1988), where waterproofing membranes are used or where deicing salts are applied less frequently, have resulted in a different set of interpretive guidelines.

In addition to the effect of environmental factors on corrosion tests, concrete repairs, e.g. adding a repair layer on an existing concrete cover, makes the evaluation and assessment of corrosion more complicated. Information on assessment of corrosion in heavily repaired concrete structures is not generally available. Much research is needed to improve understanding of the complex effects induced by the repair material and the existing substrate concrete.

This paper presents an examination of significant factors affecting the corrosion process and corrosion assessment, with the objective of providing a better and more reliable prediction of the corrosion state of reinforcing steel in concrete for different environmental exposure and conditions. A number of corrosion monitoring techniques, including half-cell potential, linear polarization, concrete resistivity and chloride ion concentration were used to evaluate the state of corrosion of reinforcement in concrete on four slab sections which had been previously removed from the old Perley Bridge located in Hawkesbury, Ontario. The concrete cover of the slabs was later removed to assess the actual corrosion state of the reinforcement and to compare it with that predicted from the measurements taken with the above techniques.

EXPERIMENTAL

The concrete slab samples

General conditions

Concrete slabs were cut from an old bridge, which was constructed with reinforced concrete and had been repaired extensively due to corrosion-induced deterioration. Four slab sections that spanned more than half of the deck width, from the sidewalk to the center of the bridge deck, were cut. Each slab sample was approximately 315 cm long (in traffic direction) and 115 cm wide, and had a concrete cover of approximately 14 cm to the top reinforcement. Reinforcement layer was composed of five 15-mm diameter longitudinal bars, spaced at 23 cm, and six 12-mm transverse bars, spaced at 45 cm. The thickness of the repair concrete overlay varied between 5 and 9 cm, depending on the location.

Tests on cores indicated that the concrete in the substrate and repair layers had relatively high compressive strength. However, very low adhesion strengths were measured between the layers. A visual inspection indicated that there was no concrete spalling at the top slab surface. There were a few horizontal cracks in concrete between the substrate and the new overlay.

Relative Humidity in the Concrete

The relative humidity (RH) measured in the concrete of four slabs at the top reinforcement level was relatively high during a monitoring period of half a year, with values above 91 % in slab 1 and 95 % in slabs 2, 3 and 4. Tap water was kept on the slabs or wet/dry cycled bi-weekly for two months in order to simulate the environmental condition to which a bridge slab is exposed to during service. The RH at the top reinforcement level increased by only 1 to 2 % due to water conditioning over the entire monitoring period, which is considered fairly negligible.

Chloride Ion Permeability and Carbonation

Chloride ion permeability in the concrete cover was low as indicated by the count of electrical charges (between 1315 and 1922 Coulombs after 6 hours) that passed through cores taken in the repair layer. The measurement was carried out according to the ASTM 1202-97 procedure (ASTM 1202-97).

There was no carbonation detected. This may indicate that carbonation was negligible at the bridge or that the repair layer had been installed in recent years.

Electrochemical measurements

A saturated copper/copper sulfate reference electrode (CSE) and a Fluke multimeter 867B with an input impedance higher than 1,000 M Ω were used to measure the half-cell potentials following the procedure provided in ASTM C876-99. The measurements were made every 45 cm in the longitudinal direction and 23 cm in the transverse direction of the slabs.

Corrosion rate measurements were made using Sensor A of the GECOR6 unit developed by GEOCISA (Feliu, Gonzalez, Feliu & Andrade, 1990). The unit uses an external guard ring to confine the applied electrical current to a known rebar area (Rodriguez, Ortega, Garcia, Johansson & Petterson, 1994). The corrosion rate was calculated by using a Tafel slope of 26 mV/decade for this device (Liu & Weyers, 1998).

Resistivity measurements were made using Sensor B of the GECOR6 unit. Before each test, the concrete surface was wetted and two to three readings were taken and then averaged at each location.

Additional experiments have also been carried out in an electrochemical cell. The electrode potentials with N₂ or O₂ bubbling were measured and recorded by means of Solartron 1287 with CorrWare software. Samples of reinforcing carbon steel bar were machined to 8 mm in diameter and embedded in Epofix resin in order to ensure a reproducible and well defined surface area. The working surfaces of electrodes had a final polish using #600 silicon carbide sand papers then placed in a three-compartment electrochemical cell and immersed in a saturated calcium hydroxide synthetic pore solution with a pH of 12.6. The corroded electrode surface was created by wetting the electrode using tap water in the air for more than 12 hours prior to immersing in the electrochemical cell. The cells were deaerated and oxygenated by bubbling high purity N₂ or O₂ gas through the solution.

Visual inspection and rating of reinforcement corrosion

After completion of the corrosion measurements, the concrete cover on the top layer of the reinforcement was removed with a jackhammer to expose the top reinforcement for visual inspection and corrosion rating. The state of the reinforcing bars was then carefully rated (at every location where corrosion measurements were taken) into one of three corrosion levels as shown in Fig. 1. Level 1 is for a bar with no visible rust products on the surface, which is probably still in a passive condition. Level 2 is for a bar with a little rust at the surface. Level 3 is for a bar on which a thick rust product had built-up. It is important to mention that the corrosion rating was only based on the state of corrosion visible on the top surface of the first layer of reinforcement. Pitting corrosion, for instance, was not taken into account since it is often not easily observed by the naked eye.



Figure 1. Rebar samples representing the 3 levels of corrosion observed.

RESULTS AND DISCUSSION

Half-Cell Potential of Reinforcing Steel in Concrete

The half-cell potential or corrosion potential of a steel bar is an indication of the probability of corrosion activity in that location. The voltage reading between a standard half-cell and a steel bar is compared to guideline values (ASTM C876-99), which have been empirically developed to indicate relative probabilities of corrosion activity. Evaluation of a large number of closely spaced half-cell potentials taken on a structure is often necessary to evaluate the probability of corrosion of the reinforcing steel in concrete.

Half-cell potentials of the reinforcement in the four slabs were plotted in the form of an equipotential contour map. A representative set of data is shown in Fig. 2a for slab 2 and Fig. 2b for slab 3. The results of the visual corrosion inspection and rating of the corrosion state after removal of the concrete cover are plotted in Fig. 3 for the same slabs.

According to ASTM C876-99, there is a 90% probability of reinforcement corrosion if half-cell potentials are less than -350 mV vs. Cu/CuSO_4 . The results of the half-cell potential survey show that most potentials on slabs 1, 3 and 4 are more negative than -350 mV. According to the guideline, these slabs would all be rated with high probability of corrosion, but actually slabs 1 and 2 were found to be mostly in good condition on the basis of the visual corrosion inspection. This disagreement is not due to the potential shift of reference electrodes since the Cu/CuSO_4 reference electrodes were compared with other reference electrodes regularly. This confirmed that the interpretation of half-cell potential results, based on the numeric guidelines suggested by the ASTM C876 standard, is unreliable for these samples because the particular environmental conditions involved, mainly the thicker concrete cover, are not taken into account by the guidelines. As noted in the standard, the interpretation of half-cell potentials under conditions where the concrete is saturated with water, where chloride concentration is high and under many other conditions, requires modification based on the knowledge of the particular corrosion conditions.

Looking at the relative half-cell potential values, they were somewhat consistent with the visual inspection results. The areas exhibiting more negative potentials are usually indicative of higher probability of corrosion. In slab 2 the two edges have more negative potential value than rest of the slab.

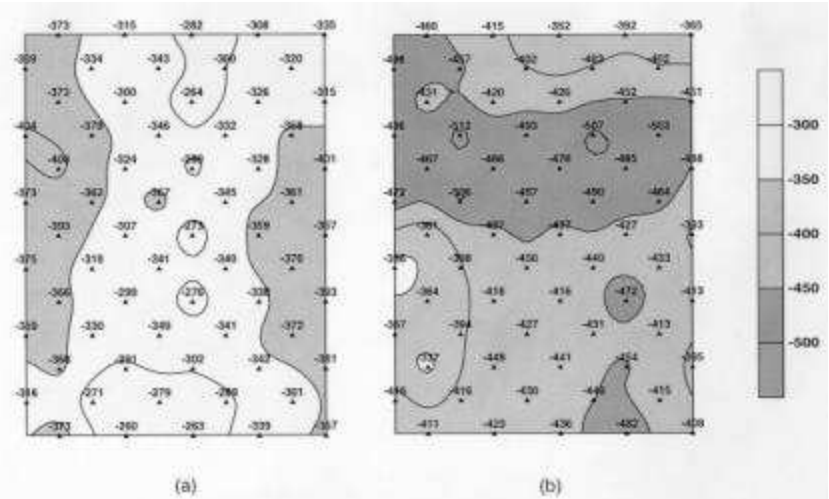


Figure 2. Equipotential contour plots measured on slab 2 (a) and slab 3 (b). The potentials are vs. CSE.

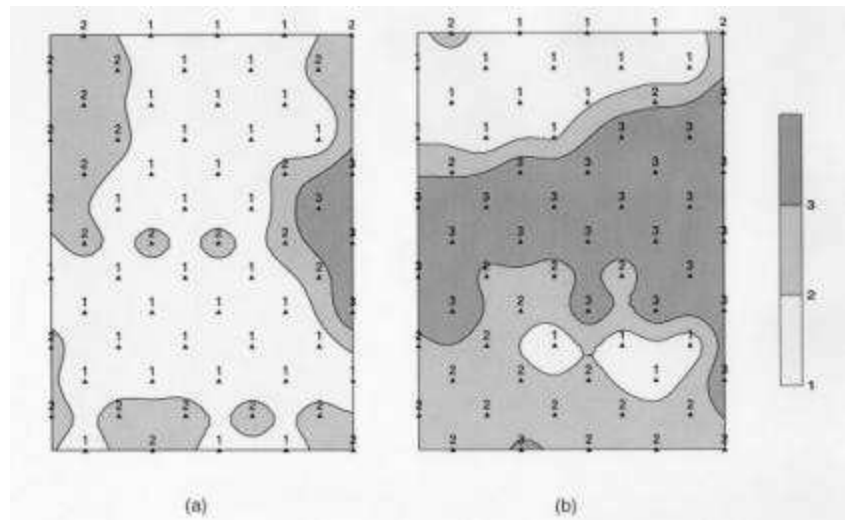


Figure 3. Rebar corrosion states rated according to the visual inspection after the removal of the concrete cover in slab 2 (a) and slab 3 (b)

These areas were found to be more corroded by visual inspection. Also in slab 3, the part of top half which has the most negative potential values also has the worst corrosion condition.

The Effect of Oxygen on the Half-Cell Potential of Reinforcing Steel

Half-cell potentials are sensitive to the ambient environment, especially oxygen concentration. Usually, a decrease in oxygen can drive the half-cell potential significantly towards more negative values. Completely water-saturated concrete can lead to oxygen starvation, resulting in potential values more negative by several hundred millivolts (Vassie, 1991), (Naish, Harker & Carney, 1990). Fig. 4 shows the continuous half-cell potential monitoring curve of a rebar in concrete prism with a 5.7 cm concrete cover that has been immersed in tap water for 16 hours. All sides of this concrete prism were sealed using plastic sheets with only the topside exposed to air for water evaporation. This test was carried out in a room with a relative humidity of 50% and a temperature of 23°C. The half-cell potential was close to -0.65 V for more than 2000 minutes, then gradually shifted to -0.45 V vs. CSE as the concrete cover became dryer. This demonstrates clearly that water-saturated concrete can lead to a significant half-cell potential shift towards negative potential. It took almost two days (more than 2800 min) for the water to evaporate to the condition under which the half-cell potential could shift back to its original value (before being immersed in the tap water).

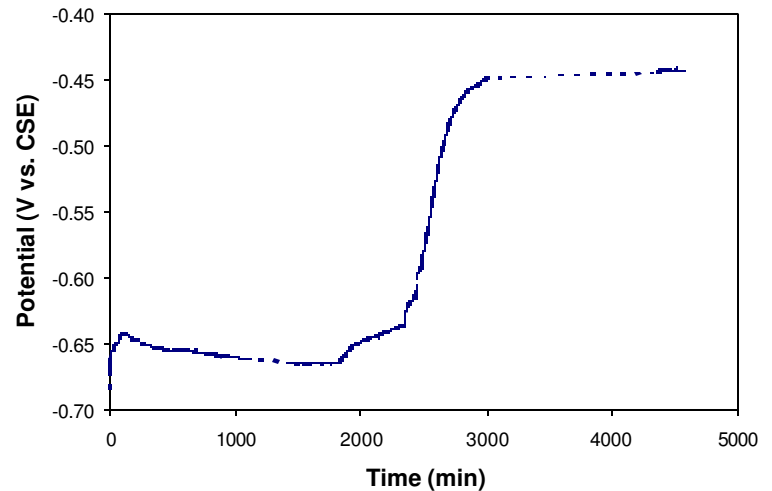


Figure 4. Half-cell potentials measured on rebar steel in concrete prism after being immersed in tap water for 16 hours.

The effect of oxygen concentration on half-cell potentials can also be demonstrated by the potential curves (Figure 5) obtained from experiments carried out in an electrochemical cell. Two electrodes (one was polished and the other was corroded) were immersed in the same cell containing saturated calcium hydroxide solution. The potentials were -0.443 and -0.760 V vs. CSE for passivated and corroded electrodes respectively when oxygen was purged by bubbling N_2 through the solution ($0 < T < 70$ min in Figure 5). The potentials shifted to -0.21 and -0.22 V vs. CSE by bubbling oxygen through the solution ($T = 360$ min). The potentials then shifted back close to their original values by bubbling N_2 through the solution again. The potential shift was more significant at the corroded steel surface than on the passivated surface. When the cell was opened to air, the potentials on these two electrodes, after reaching stable values, were slightly more negative than the potentials under the condition of bubbling O_2 (see two horizontal lines at the top left). This is because the oxygen concentration in the solution was lower when bubbling was stopped. The right-hand side of figure 5 shows the potentials on the corroded electrode after the addition of 3.5%

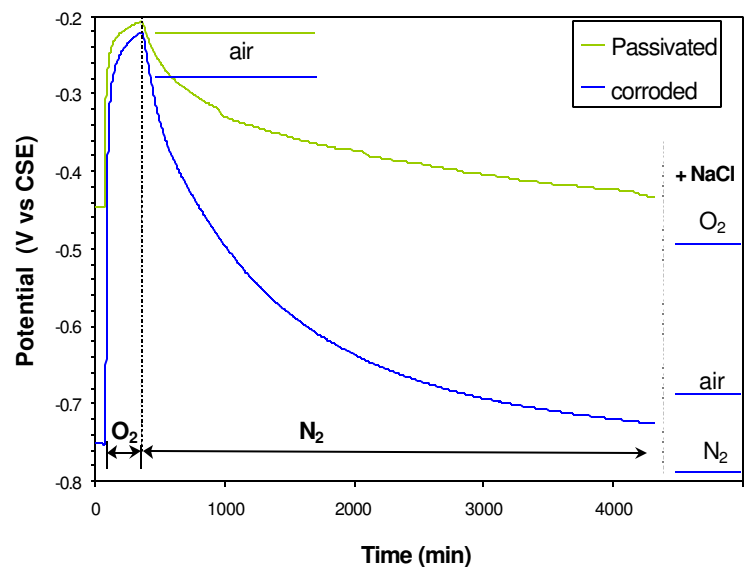


Figure 5. Half-cell potentials measured at passivated and corroded rebar electrodes in an electrochemical cell with N_2 or O_2 bubbling.

NaCl. The potentials shifted to more negative values under all three conditions (−0.5 V under O₂ bubbling, −0.69 V when the cell was opened to air and −0.79 V vs. CSE under N₂ bubbling). The Metal dissolution rate was increased by the addition of 3.5% NaCl therefore reducing the half-cell potential (as discussed further on).

Fig. 6 shows how oxygen concentration can affect the electrode potentials. The corrosion reactions of the reinforcement under conditions of access to air can be written as follows:



The product of reaction, which is ferrous hydroxide, is commonly oxidized further to magnetite (Fe₃O₄) or hydrated ferric oxide (FeOOH), i.e. rust. Considering the anodic and cathodic reactions separately, Equation (1) becomes:



and



Under conditions of no access to air (de-aerated), the reaction that shown in Equation (3) becomes reduction of water represented by:



Whenever spontaneous corrosion reactions occur, i.e. an open-circuit, all the electrons released in the anodic reaction are consumed in the cathodic reaction and no excess or deficiency of electrons can arise. The metal then normally takes up a more or less uniform electrode potential, often called the mixed or corrosion potential (E_{corr}).

Under air access conditions, the cathodic reaction is an oxygen reduction (line AA' in Fig. 6). The cathodic and anodic partial-reaction rates (line CC') are electrically equivalent at the corrosion potential, E₁, and the corresponding current, I₁ provides an electrical representation of the common rates of the anodic and cathodic partial-reactions at that potential (Shreir, Jarman & Burstein, 1994).

If the concrete cover is saturated by water, oxygen is not freely available at the metal surface because O₂ is not very soluble in aqueous solutions (ca. 10 ppm in cool seawater, for example). The cathodic reduction rate is controlled by the rate of arrival of oxygen at the metal surface and is significantly diminished. The cathodic reaction rate then changes from line AA' to line BB'. The cathodic and anodic reaction rates will have a new equivalent at the corrosion potential, E₂, and the corresponding current I₂. Because of the diminution in oxygen concentration, the corrosion potential will change from E₁ to the more negative value E₂.

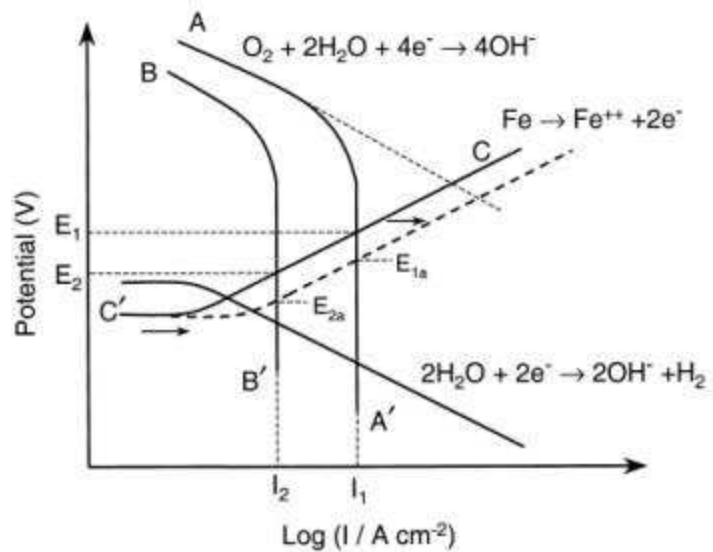


Figure 6. Polarization diagram showing the corrosion potentials and currents when the cathodic process is under mass transfer control.

When the anodic metal dissolution rate increases, the line CC' shifts to the right-hand side (dashed line). The cathodic and anodic reaction rates are thus equivalent at the corrosion potential, E_{1a}, under air

access condition and E_{2a} , under O_2 diminished condition. The corrosion potential decreases by increasing the rate of the metal dissolution.

The slab samples tested in this study had a concrete cover of 14 cm to the top reinforcement. The relative humidity at the top layer of the concrete might have changed with the ambient conditions but the RH at the reinforcement level was always very high during the test period ($> 95\%$ in slabs 2, 3 and 4, and $> 91\%$ in slab 1). Under these RH conditions, most pores in the concrete are saturated with water and the transfer of O_2 through the concrete pores to the reinforcement takes place almost entirely through liquid-phase diffusion. Therefore the concentration of oxygen was reduced and the corrosion potentials (half-cell potentials) shifted to more negative values, leading to incorrect predictions when ASTM guidelines were used.

The cumulative frequencies of half-cell potential values, calculated for the four slabs, are plotted in Fig. 7. This shows clearly that the half-cell potentials in slabs 1 and 2 were less negative while the potentials in slabs 3 and 4 were more negative. This indicates that the corrosion condition is more severe in slabs 3 and 4 than in slabs 1 and 2. This is consistent with the ratings from visual inspections.

Fig. 8 shows the cumulative frequencies of half-cell potentials at various corrosion levels. The distribution of potential ranges, corresponding to the corrosion rating, can be seen clearly, i.e. the potential values are distributed in less negative potential ranges for less corroded bars (level 1), while the potential values are dispersed over more negative potential ranges for the more corroded reinforcing bars (level 3).

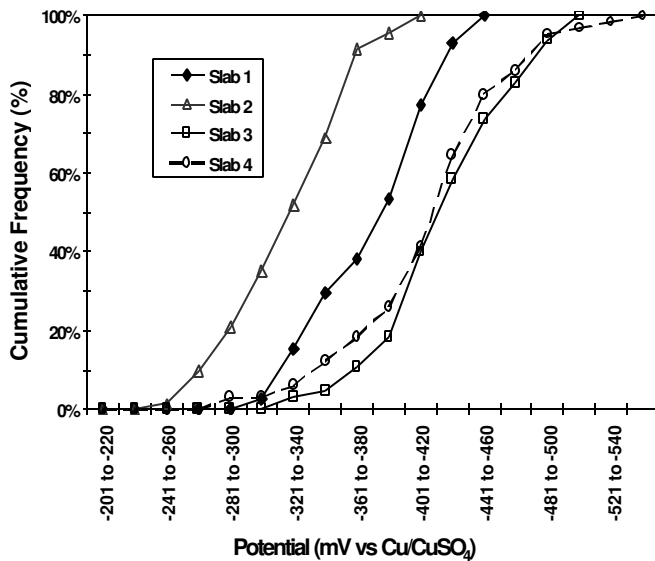


Figure 7. Cumulative frequency of half-cell potential vs. potential measured on the four slabs.

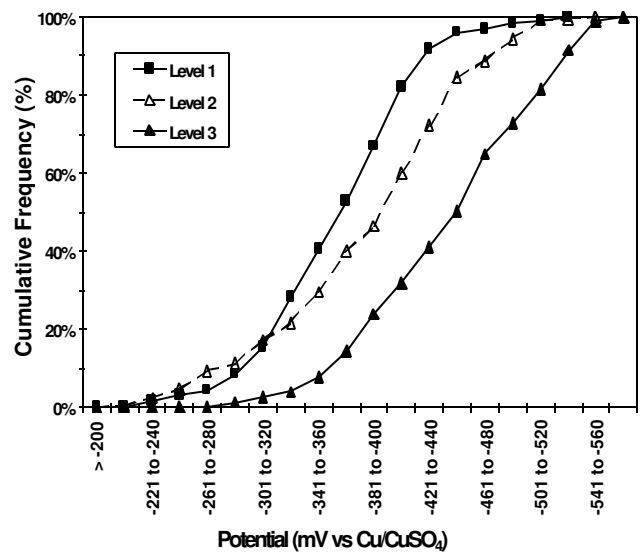


Figure 8. Cumulative frequency of half-cell potential vs. potential calculated for the three levels of corrosion.

Rate of Corrosion of Reinforcement

The linear polarization technique was used to determine the corrosion rate, i_{corr} , of reinforcing steel in the concrete, based on the following Stern-Geary equation:

$$\left(\frac{\Delta E}{\Delta i} \right)_{E_{corr}} = - \frac{b_a b_c}{2.3 i_{corr} (b_a + b_c)} \quad (5)$$

$$i_{corr} = K \left(\frac{\Delta i}{\Delta E} \right) \quad (6)$$

The values of b_a and b_c are the Tafel slope constants of the partial anodic and cathodic polarization curves and can be deduced by correlating values of potential and current ($\Delta E/\Delta i$) measured on the

sample. The K value is likely to be inaccurate and/or to change markedly as the state of corrosion in the concrete changes (temperature, moisture and chloride contents, etc.). This inaccuracy can become even bigger when the electrode surface is passivated. For simplicity, a single value (between 26 and 52 mV) is often used to calculate the corrosion rate. Practical experience with this technique has shown that in some simple electrolyte solutions, reasonably good correlation is achieved between the corrosion rate deduced by linear polarization measurements and the rate measured on corroding coupons.

The corrosion rate is a time indicator. That is to say, the corrosion information obtained is indicative of the conditions at the time of measurement and may change in a matter of days or even hours as temperature, oxygen content and moisture change. The most active corrosion may not, in fact, be occurring at the time of measurement. Continuous or intermittent monitoring over a period of time gives a more reliable appraisal of the situation. The corrosion rate is also significantly affected by the kinetic of the electrochemical reaction of the electrode. Hence, prediction of future corrosion activity must include an evaluation of several dynamic environmental factors.

Over the years, criteria have been developed from field and laboratory investigations for evaluating reinforcement corrosion based on the corrosion rate (Rodriguez, Ortega, Garcia, Johansson & Petterson, 1994). Although the criteria is useful for identifying the degree of corrosion activity of the steel, conversion into metal section loss, based only on a rate measured at a given time, is not recommended, since corrosion rates are usually not constant in time and do not follow a specific pattern.

Corrosion rates were measured at various locations on the slabs based on the linear polarization method, and are shown in Fig. 9. The corrosion current densities in slabs 1 and 2 correspond to the category of

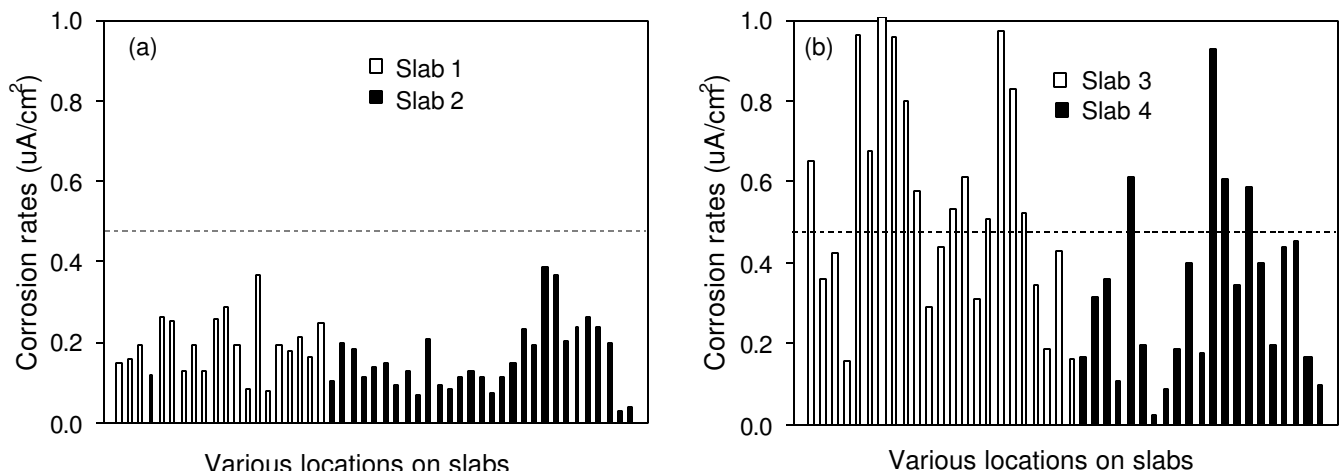


Figure 9. Corrosion current density measured on the slabs 1 and 2 (a) and slabs 3 and 4 (b).

low corrosion rate ($< 0.5 \mu\text{A}/\text{cm}^2$). The corrosion rates obtained for slabs 3 and 4 were larger and varied significantly at different locations, indicating that corrosion on these slabs was quite active (moderate to high corrosion rates). This agrees very well with the results of the visual inspection.

In the less corroded areas of slabs 3 and 4, some metal surface was very likely under the active/passive transition condition or under localized (pitting) corrosion. Although this state of corrosion is very difficult to identify by visual inspection, measured currents can be used to detect corrosion pitting (Hladky, Lomas, John, Eden, & Dawson, 1984). It has been reported (González, Andrade, Alonso & Feliú, 1993) that in the case of localized pitting, corrosion rates can be 5 to 10 times the regular corrosion rate. In severely corroded areas, the corrosion rate is probably dependent on the availability of the oxygen or the extent of corrosion product build up. The current density may not necessarily be large at the time of measurement.

In chloride contaminated concrete, corrosion often starts as pitting. When this type of corrosion occurs, the corrosion current can at first be very high; however, with time, the current could change depending on the activity of the cell, the build up of corrosion products on the steel surface and the availability of oxygen. Because of the natural fluctuation of the corrosion rate, it is more reliable to use the corrosion rate to locate the active areas on the structure instead of evaluating the overall loss of material or predicting the presence of badly corroded bars, unless constant monitoring or frequent measurements are performed.

Relation between Corrosion Potential and Corrosion Current

The measurement of corrosion potential, E_{corr} , is the method most frequently used in field tests because of its simplicity. From these measurements, contour maps of potentials are usually drawn in order to reveal those areas that are most likely to be undergoing corrosion. However, such measurements have a rather qualitative character and can be affected by many factors, as mentioned before.

It was found that the plot of the corrosion potential, E_{corr} , versus the logarithm of the corrosion current, i_{corr} , determined by the linear polarization method shows that there is poor correlation between E_{corr} and i_{corr} values for these slabs. A similar finding was also reported by Felú et al. (Feliú, González & Andrade, 1996). The poor correlation obtained is probably due to current fluctuation at the corrosion active area and shifts in potential due to change of oxygen concentration at the surface of the reinforcing steel.

Consideration of both the half-cell potential values and the results of corrosion rate measurements together can, in many cases, facilitate the interpretation of the half-cell potential results and provide more reliable evaluation of the state of reinforcement corrosion (Gu, Carter, Beaudoin & Arnott, 1996). In order to demonstrate this point, two specific examples from this study are given as follows:

1. On slabs 1 and 2, the half-cell potentials, with readings more negative than -350 mV, should not be interpreted as high probability of corrosion because the corrosion rates were low and stable. In this case, the shift in half-cell potential readings towards more negative values should be attributed to low oxygen concentration or high humidity.
2. On Slabs 3 and 4, the potential readings were generally more negative than -450 mV (much negative than -350 mV), suggesting a high probability of corrosion. Taking into consideration the high corrosion rates measured and their significant fluctuations from one location to another, the prediction of active corrosion can be made with confidence. In these slabs, the section with more negative potentials was more corroded, as was confirmed by visual inspection.

Electrical Resistivity of the Concrete Cover

The resistivity of concrete is related to moisture and the content of charged ions and their mobility. Measuring conductivity (or resistivity) gives a measure of how easily corrosion current flows as a result of local potential differences caused by the state of corrosion. It is typically about 10,000 ohm-cm, but can be as low as a few hundred ohm-cm or as high as 100,000 ohm-cm. Resistivity measurements can thus give valuable information for the interpretation of electrode potential results made under the same conditions.

In this work a GECOR6 unit was used to measure resistivity in concrete. This unit applies a pulse signal between the sensor and a reinforcing bar and measures the iR drop between the reference electrode and the bar. In this way, the polarization potential at the sensor and the rebar surface is eliminated. However, the GECOR6 instrument has its limitations in measuring the resistivity in the concrete, as discussed in the following paragraphs.

The distribution and size of the aggregates can affect measurements of concrete resistivity. Readings of resistivity also fluctuate when the measurement probe is moved from one place to another. The data analysis has, then, to rely on a relatively large number of representative measurements that must be treated by statistical analysis.

It is also important to note that the GECOR6 unit was designed to measure the resistivity in a concrete cover that has a normal thickness of 50 - 60 mm, based on given current distribution. When the thickness of the concrete cover is significantly larger (as in this study), the condition of the top layer of concrete has a larger influence on the resistivity measurement than the condition of the concrete layer near the reinforcement level.

The resistivity values measured on the four slabs in June, September and December are plotted as cumulative frequency vs. concrete resistivity in Fig. 10. The results show that the resistivity measured in June has the largest value while the resistivity obtained in September is smallest. This is because the measurements carried out in June were conducted after 2 months of dry conditions. The September measurements were performed after 2 months of continuous wet condition, while the measurements carried out in December were done after 2 months of biweekly wet-dry cycles. The moisture content in the top concrete layer was lowest in June and highest in September, resulting in a corresponding change of resistivity, since it is related to the moisture content in the concrete.

Fig. 11 shows the cumulative frequency vs. resistivity at various locations on reinforcing bars having different levels of corrosion. These levels of corrosion at the reinforcement were defined after the concrete cover was removed. For the data obtained in June (Fig. 11a), it was found that differences in resistivity between corrosion levels are quite small due to the contribution of the high resistivity of the top layer of concrete. Larger differences in resistivity can be clearly observed in the results obtained in September (Fig. 11b) and especially in December (Fig. 11c). In these measurements, the concrete resistivity was not dominated by the top layer of concrete since the top layer concrete was thoroughly wetted by the water so that the resistivity in this concrete layer was reduced. Therefore the resistivity in the concrete layer near the reinforcement level can have

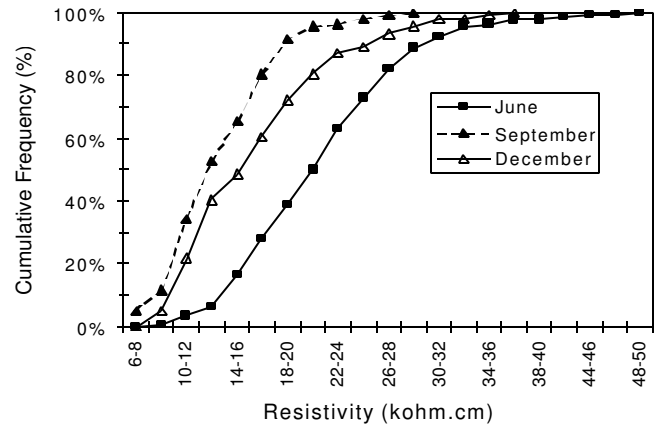


Figure 10. Cumulative frequency of concrete resistivity vs. resistivity calculated for June, September and December, respectively.

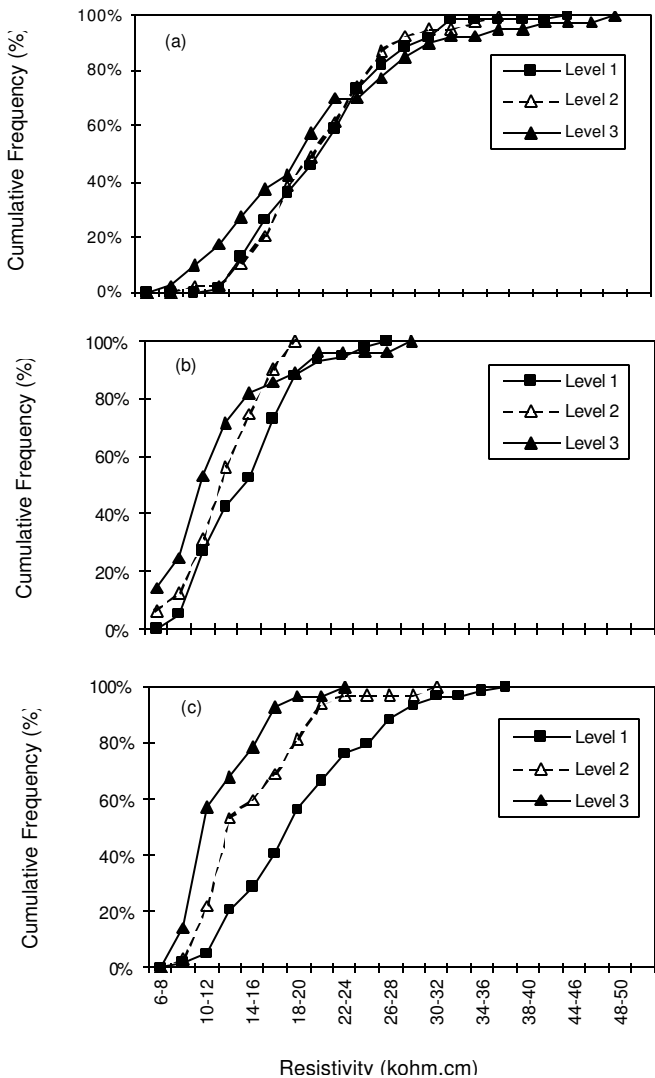


Figure 11. Cumulative frequency of concrete resistivity vs. resistivity calculated for the three levels of corrosion in June (a), September (b), and December (c).

a relatively larger contribution and be identified in the resistivity measurements. In these surveys, the most corroded bars (level 3) were located in the areas where the concrete resistivity was low while the less corroded bars (level 1) were found in areas having a high concrete resistivity. In the later area the electrically charged ions have more difficulty moving through the pore liquid, thus reducing the corrosion rate.

Chloride Content

Fig. 12 presents the average profile of the chloride ion content measured on 50 mm diameter cores from the top surface down to the reinforcement level in each slab. The chloride ion content ranged from 0.0 to 0.6 % by weight of concrete. Regardless of the slab number or the depth at which measurements were made, the chloride content exceeded (except for one measurement) the 0.02 % threshold limit over which a concrete is considered significantly contaminated by chloride ions (Hope & Ip, 1987). For each slab, the chloride content reached a maximum value at a depth of 10 mm from the top surface and decreased to lower concentrations (but still excessive) towards the reinforcement level in the old concrete. Slightly lower chloride contents were found at the surface than at the 10 mm depth due to effect of rain washing out chloride ions at the slab surface.

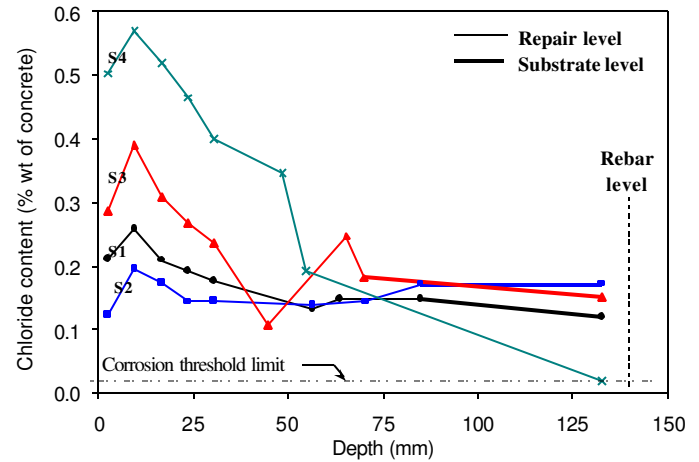


Figure 12. Chloride content measured on 50 mm diameter cores.

Slabs 3 and 4 had much larger chloride ion contents than slabs 1 and 2 in the repair layer. This may be related to the original location of the slabs on the bridge. Slabs 1 and 2 were closer to the side of the deck, in a high traffic area, where cars probably had splashed the salts away. Slabs 3 and 4 were located at the center of the deck in a lower traffic-density area, allowing the salts to have a chance to remain there longer. This is consistent with the results of visual inspection and the electrochemical measurements.

The lack of proportionality between the chloride levels in the old concrete and that in the repair layer is quite unexpected. However, the measurements performed in the old concrete should be regarded as less precise than those taken in the repair layer. The reason is that the much larger aggregates in the old concrete may have introduced larger errors in the determination of the chloride content, which was based on the weight of concrete.

CONCLUSIONS

Adequate evaluation of the state of reinforcement corrosion in bridge concrete slabs is complex and requires extensive experience and knowledge, as well as the simultaneous consideration of a variety of interrelated factors, such as corrosion potential, corrosion rate, electrical resistivity, environmental conditions.

Half-cell potential of reinforcement can be affected significantly by oxygen concentration at the steel surface. When the concrete cover is thick due to extensive repair or saturated with water, the transfer of O_2 through the concrete becomes difficult, leads to the reduction of oxygen concentration and causes the corrosion potential to shift significantly towards more negative values. The interpretations of half-cell potentials, based simply on the numerical guidelines in the ASTM C876 standard, can result in unreliable predictions of reinforcement corrosion.

A statistical analysis of a large number of half-cell potential readings, measured under similar conditions, showed that the relative state of corrosion of concrete slabs could be predicted reasonably well. The slab sections exhibiting more negative potentials were usually more corroded.

High readings and significant fluctuations, from one location to another, in the corrosion rates measured by linear polarization are shown to be a good indication of active corrosion. It can be used to verify the corrosion active areas for the corrosion prediction by half-cell potential.

The resistivity of the concrete cover, measured by means of GECOR 6, was significantly affected by the moisture conditions at the top layer of concrete. The corrosion of reinforcement is related to the concrete resistivity. It can be used to assist the prediction of state of corrosion if the measured resistivity is that contributed by concrete near the reinforcement level.

ACKNOWLEDGEMENTS

The National Research Council Canada (NRC) wishes to acknowledge the financial support of Public Works and Governmental Services Canada (PWGSC), with special thanks to Dr. M. S. Cheung, Director Technology & Environment at PWGSC for his interest and support. The assistance of Dr. Daniel Cusson, Mr. Gordon Chan and Mr. Ted Hoogeveen of NRC is also greatly appreciated.

REFERENCES

- ASTM C1202-97, (1997), *Standard Test Method for Electrical Indication of Concrete's Ability to Resist Chloride Ion Penetration*, ASTM, Philadelphia.
- ASTM C876-99 (1999): *Standard Test Method for Half-cell Potentials of Reinforcement in Concrete*, ASTM, Philadelphia.
- Elsener B. and Bohni H., (1990), *ASTM STP 1065*, N. S. Berke et al., ed., ASTM, Philadelphia, 143.
- Feliú S., González, J. and Andrade C. (1996), "Techniques to Assess the Corrosion Activity of Steel Reinforced Concrete Structures," *ASTM STP 1276*, Berke, N. et al., Eds., American Society for Testing and Materials, 107.
- Feliu S., Gonzalez J. A., Feliu S. Jr. and Andrade C., (1990), *ACI Materials Journal*, Sep.-Oct., 457.
- González, J., Andrade, C., Alonso P. and Feliú S. (1993), *Progress in the Understanding and Prevention of Corrosion*, Costa, J. and Mercer A., Eds, The European Federation of Corrosion, 629.
- Gu, P., Carter, P., Beaudoin, J.J. and Arnott, M. (1996), "Validation of half-cell potential data from bridge decks", *Construction Repair*, **10**(3), 18-20.
- Hladky, K., Lomas, J., John, D., Eden, D. and Dawson J. (1984), *In Proceedings of the Conference on Corrosion Monitoring and Inspection in the Oil, Petroleum and Process Industries*, London, 211.
- Hope, B. B. and Ip, A.K.C. (1987), "Chloride Corrosion Threshold in Concrete," *ACI Materials Journal*, July-August, **84**(4), 306-314.
- Liu T. and Weyers R. W., (1998), *Cement and Concrete Research*, **28**(3), 365-379.
- Naish C. C., Harker A. and Carney R. F. A., (1990), Concrete inspection: "Interpretation of potential and resistivity measurements", *Proc. Corrosion of Reinforcement in Concrete*, Elsevier Applied Science, 314-332.
- Raherinaivo A., (1988), "Contrôle de la corrosion des armatures dans les structures en béton armé", *Bulletin De liaison des Laboratoires des Ponts et Chaussées*, 158, Nov./Dec., 29-38.
- Rodriguez, J., Ortega, L., Garcia, A., Johansson L. and Petterson K., (1994), *Proceedings of the International Conference on Concrete Across Borders*, Vol. 1, Odense, Denmark, June, 215.
- Shreir L. L., Jarman R. A. and Burstein G. T., (1994), "Corrosion", Oxford, third edition, Vol. 2, 10.7.
- Vassie P. R., (1991), *TRRL Application Guide 9*, 30.